Eur. Phys. J. A **30**, 455–460 (2006)
DOI 10.1140/epja/i2006-10142-5

THE EUROPEAN PHYSICAL JOURNAL A

Phase transition to color-flavor-locked matter and condensation of Goldstone bosons in neutron star matter

J.F. Gu[1,a], H. Guo[1,2], X.G. Li[2,3], Y.X. Liu[1,2,4], and F.R. Xu[1,2]

[1] Department of Technical Physics and MOE Laboratory of Heavy-Ion Physics, Peking University, Beijing 100871, PRC
[2] Center of Theoretical Nuclear Physics, National Laboratory of Heavy-Ion Accelerator, Lanzhou 730000, PRC
[3] Institute of Modern Physics, The Chinese Academy of Sciences, Lanzhou 730000, PRC
[4] Department of Physics, Peking University, Beijing 100871, PRC

Received: 11 August 2006 / Revised: 17 September 2006 /
Published online: 27 November 2006 –
Communicated by A. Schäfer

Abstract. Deconfinement phase transition and condensation of Goldstone bosons in neutron star matter are investigated in a chiral hadronic model (also referred as to the FST model) for the hadronic phase (HP) and in the color-flavor-locked (CFL) quark model for the deconfined quark phase. It is shown that the hadronic-CFL mixed phase (MP) exists in the center of neutron stars with a small bag constant, while the CFL quark matter cannot appear in neutron stars when a large bag constant is taken. Color superconductivity softens the equation of state (EOS) and decreases the maximum mass of neutron stars compared with the unpaired quark matter. The K^0 condensation in the CFL phase has no remarkable contribution to the EOS and properties of neutron star matter. The EOS and the properties of neutron star matter are sensitive to the bag constant B, the strange quark mass m_s and the color superconducting gap Δ. Increasing B and m_s or decreasing Δ can stiffen the EOS which results in the larger maximum masses of neutron stars.

PACS. 26.60.+c Nuclear matter aspects of neutron stars – 21.65.+f Nuclear matter – 12.38.-t Quantum chromodynamics – 95.30.Cq Elementary particle processes

1 Introduction

Neutron star matter provides astrophysical laboratories for the dense matter physics. The baryon density in the neutron star interior can exceed a few times the saturation density of nuclear matter, and the deconfinement transition from the hadronic phase (HP) to the quark phase possibly occurs in neutron stars [1,2]. Recently, it is generally accepted that the color-flavor-locked (CFL) phase [3,4] is the true ground state of matter at a sufficiently high density. In the CFL phase, quarks with three colors and flavors form Cooper pairs near the Fermi surface, and the formation of quark pairs breaks the color gauge symmetry. Nambu-Goldstone bosons [5,6] such as π^- and K^0 are the lightest degrees of freedom, emerge, and may play an important role in the CFL phase. The transition from the HP to the CFL quark phase and the effects on the properties of neutron stars have been investigated by several authors [7–11]. In fact, whether deconfinement transition from the HP to the CFL quark phase occurs and do Nambu-Goldstone bosons condensate in the CFL phase or not in neutron stars is a matter of controversy because of the lack of direct observation, therefore intensive investigations are still expected.

[a] e-mail: jianfagu@gmail.com

Recently, a chiral hadronic model has been proposed by Furnstahl, Serot, and Tang (referred to as the FST model in the following) [12]. The FST model phenomenologically respects the main features of the theorem of strong interaction predicted by QCD, *i.e.*, a nonlinear realization of chiral symmetry, broken scale invariance, and the effect of vector dominance [12]. Strong interaction plays a central role in neutron star matter, and it seems more reasonable to choose the FST model to describe the dense matter of neutron stars in the present paper. So far, the calculation of the condensation of both Goldstone bosons (π^- and K^0) in the CFL phase and its effects on the gross properties of neutron star matter has not been performed. It is very interesting to carry out those investigations systemically in this paper. Besides, we also discuss the effects of color superconductivity on the EOS and the mass-radius relation of neutron stars. The effects of the variation of the bag constant, the color superconducting gap and the strange quark mass on the deconfinement transition and on the properties of neutron star matter will be emphasized.

The rest of this paper is organized as follows. In sect. 2, the models and the basic formulae are given. The results and conclusions are presented in sect. 3.

2 Models of neutron star matter

2.1 The FST model for hadronic matter

The Lagrangian density of the FST model [12] is given by

$$\mathcal{L}=\sum_B \bar{\psi}_B\Big[i\gamma_\mu\mathcal{D}_B^\mu+g_{AB}\gamma^\mu\gamma_5 a_\mu+g_{\sigma B}\phi-\frac{1}{2}g_{\rho B}\gamma_\mu\boldsymbol{\tau}\cdot\boldsymbol{b}^\mu -M_B\Big]\psi_B-\frac{1}{4}F_{\mu\nu}F^{\mu\nu}+\frac{1}{4!}\xi(g_\omega^2V_\mu V^\mu)^2+\frac{1}{2}\partial_\mu\phi\partial^\mu\phi +\frac{1}{2}\Big[1+\eta\frac{\phi}{S_0}+\cdots\Big]\Big[\frac{1}{2}f_\pi^2\,\mathrm{tr}(\partial_\mu U\partial^\mu U^+)+m_v^2V_\mu V^\mu\Big]-H_q \times\Big(\frac{S^2}{S_0^2}\Big)^{\frac{2}{d}}\Big(\frac{1}{2d}\ln\frac{S^2}{S_0^2}-\frac{1}{4}\Big)-\frac{1}{4}\boldsymbol{G}_{\mu\nu}\cdot\boldsymbol{G}^{\mu\nu}+\frac{1}{2}m_\rho^2\boldsymbol{b}_\mu\cdot\boldsymbol{b}^\mu\,, \quad (1)$$

where $\psi_B(B=n,p,\Lambda,\Sigma^+,\Sigma^-,\Sigma^0,\Xi^-,\Xi^0)$ denote the octet fields of baryons. The self-interaction term of the vector fields with the real coefficient ξ and the cross interaction one between the scalar and the vector fields with the real coefficient η are included. $\mathcal{D}_B^\mu\equiv\partial^\mu+iv^\mu+ig_{vB}V^\mu$ is a chirally covariant derivative for baryons. The coefficient H_q represents the heavy glueball contributions. Other notations in the above formulae are the same as those used in ref. [13].

In the following we use the parameter set T3 of the FST model to perform calculations and other coupling constants are determined in the same way as in ref. [13]. By using the standard variational approach one can derive the closed nonlinear set of equations of motion for baryon, lepton and meson fields. These equations plus constraint conditions for neutron star matter can be solved self-consistently in the mean-field approximation, the properties of neutron star matter can then be described.

2.2 The color-flavor-locked quark matter

We describe the color-flavor-locked (CFL) quark phase by using the thermodynamical potential [8]

$$\Omega_{CFL}(\mu,\mu_e)=\Omega_{quark}(\mu,\mu_e)+\Omega_{GB}(\mu,\mu_e)+\Omega_l(\mu_e), \quad (2)$$

where μ is the average chemical potential of quarks. Ω_{quark} is the contribution from u, d, s quarks:

$$\Omega_{quark}(\mu,\mu_e)=\frac{6}{\pi^2}\int_0^\nu p^2(p-\mu)\mathrm{d}p-\frac{3\Delta^2\mu^2}{\pi^2} +\frac{3}{\pi^2}\int_0^\nu p^2\big(\sqrt{p^2+m_s^2}-\mu\big)\mathrm{d}p+B, \quad (3)$$

where ν is the common Fermi momentum as $\nu=2\mu-\sqrt{\mu^2+\frac{m_s^2}{3}}$, and m_s denotes the strange quark mass. Δ is the color superconducting gap which determines the binding energy of Cooper pairs in the CFL phase, and B is the bag constant. The baryon number density ρ_B^Q and the quark number densities read

$$\rho_B^Q=\rho_u=\rho_d=\rho_s=\frac{\nu^3+2\Delta^2\mu}{\pi^2}\,. \quad (4)$$

$\Omega_{GB}(\mu,\mu_e)$ [5,6] represents the contribution from the Goldstone bosons (π^- and K^0) as a result of the breaking of chiral symmetry in the CFL phase:

$$\Omega_{GB}(\mu,\mu_e)=-\frac{1}{2}f_\pi^2\mu_e^2\Big(1-\frac{m_\pi^2}{\mu_e^2}\Big)^2 -\frac{1}{2}f_\pi^2\frac{m_s^4}{4\mu^2}\Big(1-\frac{4\mu^2m_{K^0}^2}{m_s^4}\Big)^2, \quad (5)$$

where the decay constant f_π^2 and the masses of the Goldstone bosons are given by

$$f_\pi^2=\frac{(21-8ln2)\mu^2}{36\pi^2}\,, \qquad m_\pi^2=\frac{3\Delta^2}{\pi^2f_\pi^2}m_s(m_u+m_d),$$
$$m_{K^0}^2=\frac{3\Delta^2}{\pi^2f_\pi^2}m_u(m_s+m_d). \quad (6)$$

When the electron chemical potential exceeds the mass of the π^--meson, the π^--meson condensation appears in the CFL phase. Here we also consider the contribution of K^0 condensation although it is the effect of order m_s^4. The K^0-meson may condense when the condition $m_s^2/2\mu\geq m_{K^0}$ is satisfied.

The contribution from leptons is

$$\Omega_l(\mu_e)=\sum_l\frac{1}{3\pi^2}\int_0^{p_F}\frac{p^4\mathrm{d}p}{\sqrt{p^2+m_l^2}}\,. \quad (7)$$

The pressure, energy density and electric charge density (carried by the π^--meson) in the CFL phase are expressed by

$$P_Q=-\Omega_{CFL}\,, \quad (8)$$
$$\varepsilon_Q=\sum_i\mu_in_i-P, \quad (9)$$
$$\rho_e^Q=-f_\pi^2\mu_e\Big(1-\frac{m_\pi^4}{\mu_e^4}\Big). \quad (10)$$

2.3 Conditions for hadronic-CFL phase transition

The phase transition from the HP to the CFL phase occurs when the Gibbs conditions are satisfied [1,14]. This leads to the MP to appear in neutron stars. The MP lies in equilibrium:

$$P_H(\mu_n,\mu_e)=P_Q(\mu,\mu_e), \quad (11)$$
$$\mu_n=3\mu. \quad (12)$$

In the MP, the global charge neutrality condition should be satisfied:

$$(1-\chi)\rho_e^H+\chi\rho_e^Q+\rho_e^l=0, \quad (13)$$

where $(1-\chi)$ and $\chi=V_Q/(V_H+V_Q)$ are the volume fractions of the hadronic and the CFL matter in the MP. The baryon density and energy density in the MP are

$$\rho_B=(1-\chi)\rho_B^H+\chi\rho_B^Q\,, \quad (14)$$
$$\varepsilon=(1-\chi)\varepsilon_H+\chi\varepsilon_Q+\varepsilon_l\,. \quad (15)$$

Table 1. The bag constat $B^{1/4}$ (MeV), gap Δ (MeV), strange quark mass m_s (MeV), critical density of the CFL quark matter $u_{cr} \equiv \rho_{cr}/\rho_0$, critical density of the pure CFL quark core u_e, maximum masses M_{max}, corresponding radii R (km), and central densities u_{cen} of neutron stars in the FST model with the parameter set T3.

				T3				
Composition	$B^{1/4}$	Δ	m_s	u_{cr}	u_e	$\frac{M_{max}}{M_\odot}$	R	u_{cen}
Unpair quarks	190	0	150	2.16	–	1.46	13.18	6.04
CFL quark	190	80	150	2.92	6.62	1.40	15.03	4.02
CFL + π^-	190	100	150	1.74	5.26	1.05	16.01	3.02
CFL + π^-	190	80	150	2.2	6.56	1.30	15.16	3.66
CFL + π^-	190	70	150	2.56	7.16	1.38	14.85	3.96
CFL + $\pi^- K^0$	190	80	150	2.2	6.56	1.30	15.17	3.64
CFL + $\pi^- K^0$	200	80	150	5.62	–	1.49	13.76	5.20
CFL + $\pi^- K^0$	190	90	150	1.92	6.00	1.19	15.53	3.34
CFL + $\pi^- K^0$	190	80	170	2.46	6.92	1.37	14.92	3.88
CFL + $\pi^- K^0$	190	80	180	2.64	–	1.40	14.76	4.04
CFL + $\pi^- K^0$	190	80	185	2.74	–	1.41	14.67	4.14
CFL + $\pi^- K^0$	190	75	180	2.90	–	1.43	14.59	4.20

If a fixed ρ_B is given, eqs. (11)-(14) plus the equations of the HP can be solved self-consistently, and then we can obtain the volume fraction χ.

3 Results and conclusions

3.1 Results

The fractions of particles in neutron star matter are plotted in fig. 1 in the FST model with the condensation of Goldstone bosons (π^- and K^0) in the CFL phase. The physical quantities related to the properties of neutron stars are listed in table 1. It is seen that the different values of $B^{1/4}$, m_s and Δ dramatically influence the composition of neutron star matter. In figs. 1(a), (b) and (c) with $B^{1/4} = 190\,\mathrm{MeV}$, once the CFL phase emerges, the fractions of the CFL quark matter and Goldstone bosons increase rapidly. Meanwhile, the fractions of electron and muon decrease dramatically because the negative-charge meson π^- replaces them to keep the global charge neutrality in neutron star matter. In the high-density region, hadrons, leptons and π^--meson disappear and the CFL quark core with K^0 condensation forms in neutron star matter. Because the central densities of neutron stars are smaller than the critical densities of the pure CFL quark core (see fig. 1 and table 1), the pure CFL quark core is excluded and the MP exists in the center of neutron stars. In figs. 1(a) and (b), Λ and Σ^- hyperons can appear in neutron stars. No hyperons can appear in neutron stars in fig. 1(c) with $\Delta = 90\,\mathrm{MeV}$, since the critical density of the CFL quark matter is smaller than those of hyperons and the CFL quark matter suppresses the appearance of hyperons. In fig. 1(d) with $B^{1/4} = 200\,\mathrm{MeV}$, due to the emergence of hyperons, the critical density of the CFL quark matter is shifted to the higher density in the neutron star matter. Besides, Σ^+, Ξ^0 hyperons and the CFL quark matter cannot appear in neutron stars, because the critical densities of those particles are larger than the central density of the maximum neutron star.

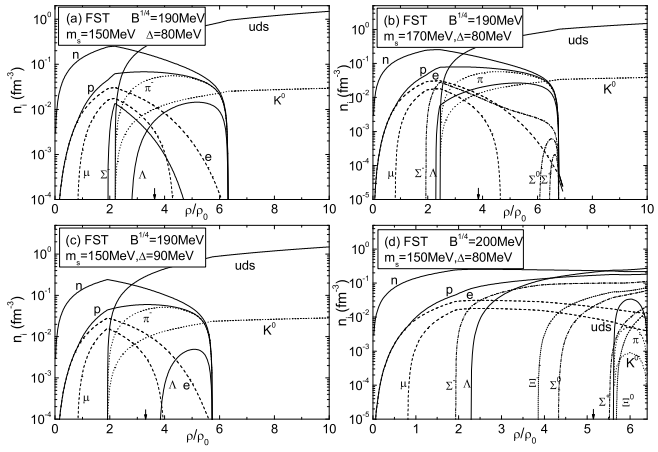

Fig. 1. The number densities n_i of various particles in neutron matter in the FST model with the parameter set T3. The short arrow at the transverse axis indicates the central density of a maximum neutron star.

The pressure as a function of energy density in neutron star matter in the FST model is plotted in fig. 2. It is shown that color superconductivity makes the equation of state (EOS) of the MP softer than that with the unpaired quark matter. However, the EOS with the CFL phase is stiffer than that with unpaired quark matter in the high-density region after the pure CFL quark core forms in neutron star matter. In the MP region, the EOS with $\Delta = 100\,\mathrm{MeV}$ is softer than the case with $\Delta = 80\,\mathrm{MeV}$, so the EOS of the MP becomes softer as increasing the gap; while in the high-density region, the EOS becomes stiffer with increasing gap. In fig. 2, we can see that the

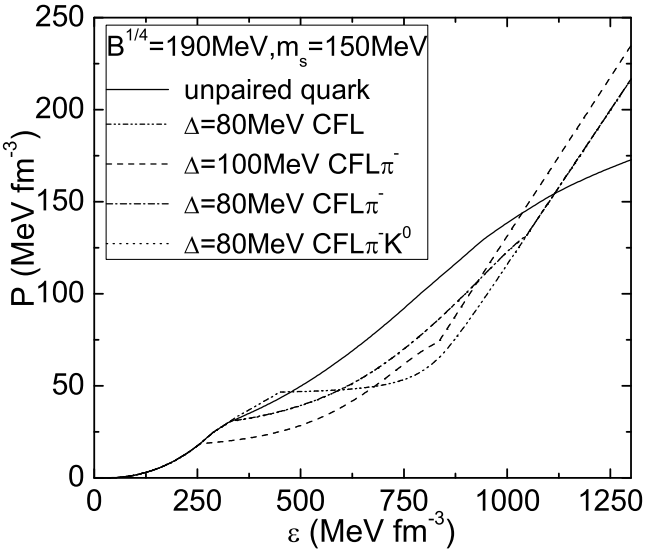

Fig. 2. Pressure P as a function of energy density ε in the FST model with the parameter set T3.

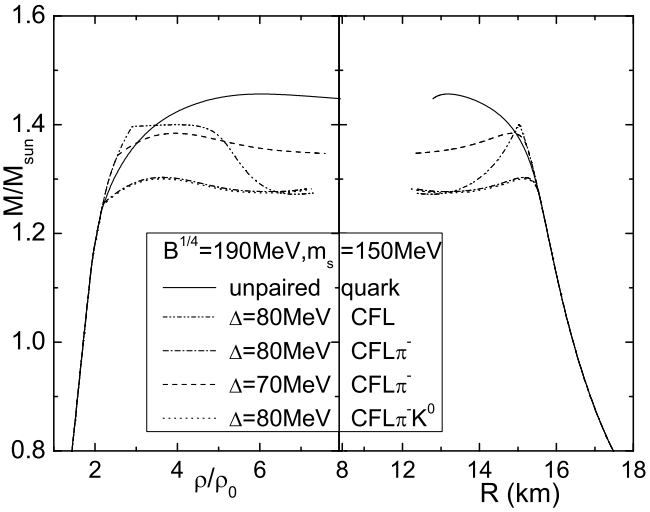

Fig. 3. The masses of neutron stars *versus* the baryon density and the mass-radius relation calculated in the FST model with the parameter set T3.

condensation of Goldstone bosons makes the pressure of the MP increase more smoothly during the deconfinement phase transition. The K^0 condensation in the CFL phase does not remarkably affect the EOS of the system since both curves for $\Delta = 80\,\mathrm{MeV}$ with CFLπ^- and CFL$\pi^- K^0$ coincide in fig. 2.

By integrating the Tolman-Oppenheimer-Vokoff equations together with the EOS of the FST model, the neutron star masses *versus* the baryon density and the mass-radius relation for neutron stars are shown in fig. 3. The bag constant $B^{1/4} = 190\,\mathrm{MeV}$ and $m_s = 150\,\mathrm{MeV}$ are taken in the quark phase. The maximum mass and radius of neutron stars with the unpaired quark phase is $1.46 M_\odot$ and 13.18 km, here $M_\odot$ denotes the mass of Sun; the maximum mass (radius) with $\Delta = 80\,\mathrm{MeV}$ of the CFL

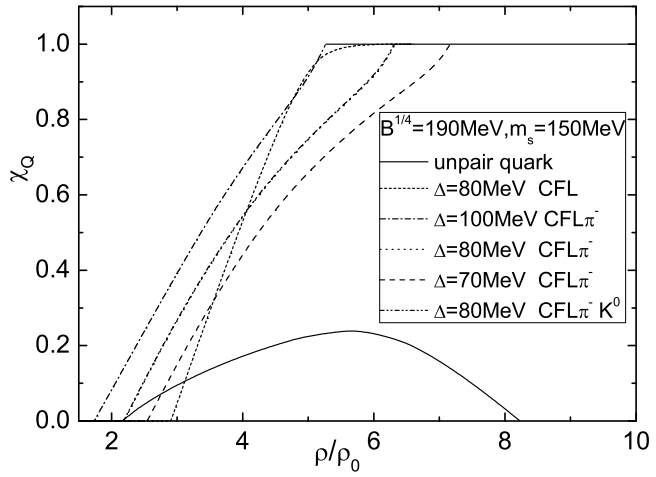

Fig. 4. The volume fraction of the quark matter *versus* the baryon density in neutron star matter in the FST model with the parameter set T3.

phase is $1.40 M_\odot$ (15.03 km). When including the condensation of the π^--meson in the CFL phase, the maximum masses (radii) with $\Delta = 80\,\mathrm{MeV}$ and $\Delta = 70\,\mathrm{MeV}$ are $1.30 M_\odot$ (15.16 km) and $1.38 M_\odot$ (14.85 km) (see fig. 3 and table 1). Therefore, we can see that color superconductivity and the condensation of Goldstone bosons make the maximum masses of neutron stars decrease because the EOS becomes softer than that with the unpaired quark matter in the MP. Moreover, the maximum masses of neutron stars decrease with the increasing values of the gap. The K^0 condensation in the CFL phase has no remarkable contribution to the mass and radius of neutron stars.

Figure 4 depicts the volume fraction of the quark phase as a function of the baryon density in neutron star matter in the FST model. It is shown that the volume fraction of the unpaired quark matter increases in the low-density region and drops in the high-density region; the critical density of CFL phase with $\Delta = 80\,\mathrm{MeV}$ is 2.92 ρ_0 and the MP phase ends at 6.62 ρ_0. Including the π^--meson condensation in the CFL phase, the MP with the gap $\Delta = 100, 80$ and 70 MeV begins at 1.74, 2.2 and 2.56 ρ_0, respectively, and ends at 5.26, 6.56 and 7.16 ρ_0 (see fig. 4 and table 1). One can see that the condensation of Goldstone bosons makes the critical densities shift to the lower densities and the appearance of the CFL quark matter turns out to be easier. Moreover, the critical densities of the CFL quark matter become smaller with increasing values of the gap.

The bag constant B, the strange quark mass m_s and the color superconducting gap Δ are the free parameters of the CFL quark model. Now, we investigate the influences of the free parameters on the EOS and properties of neutron star matter. The results are displayed in fig. 5. It is found that with the fixed Δ and m_s, the EOS with $B^{1/4} = 200\,\mathrm{MeV}$ is stiffer than that with $B^{1/4} = 190\,\mathrm{MeV}$ in the MP. So keeping the gap and the strange quark mass fixed, the EOS becomes stiffer by increasing the bag constant. If we fix the bag constant and the mass of strange quark, the EOS with $\Delta = 90\,\mathrm{MeV}$ is softer than that with

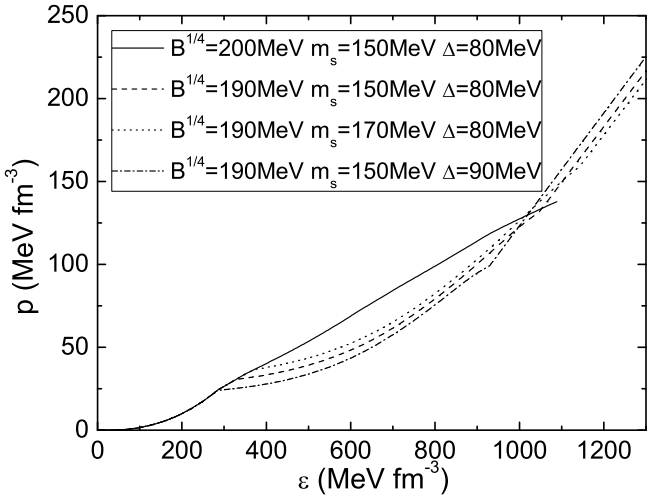

Fig. 5. Pressure P as a function of the energy density ε of the neutron star matter with $B^{1/4} = 190\,\text{MeV}$ and $200\,\text{MeV}$. $\Delta = 80\,\text{MeV}$ and $90\,\text{MeV}$ and $m_s = 150\,\text{MeV}$ and $170\,\text{MeV}$ are taken in the CFL quark model.

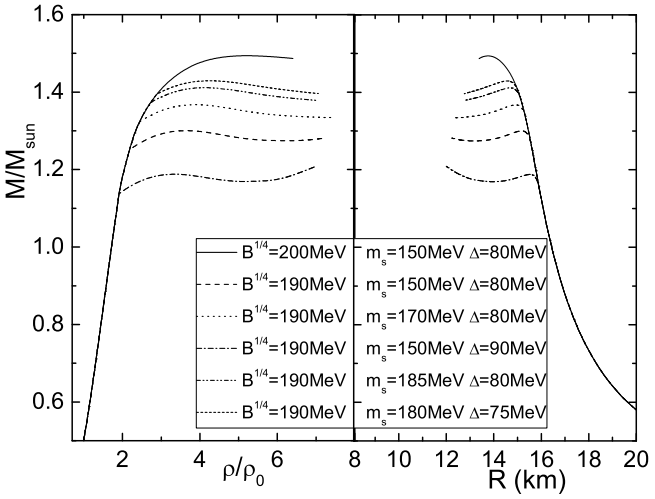

Fig. 6. The masses of neutron stars *versus* the baryon density and the mass-radius relation with different values of B, m_s and Δ.

$\Delta = 80\,\text{MeV}$, one can conclude that the EOS becomes softer with increasing gap. In the cases with the fixed bag constant and gap, the EOS with $m_s = 150\,\text{MeV}$ is softer than that with $m_s = 170\,\text{MeV}$. Therefore, increasing the strange quark mass stiffens the EOS.

The neutron star masses *versus* the baryon density and the mass-radius relation for neutron stars with different values of B, m_s and Δ are presented in fig. 6. We can see that with the fixed strange quark mass and gap, the maximum masses of neutron stars with $B^{1/4} = 200\,\text{MeV}$ are larger than those with $B^{1/4} = 190\,\text{MeV}$ (see fig. 6 and table 1) because the EOS with the larger bag constant is stiffer. Hence, the maximum masses of neutron stars increase with increasing bag constant. When we fix the bag constant and the strange quark mass, the maximum masses of neutron stars with $\Delta = 90\,\text{MeV}$ are smaller than those with $\Delta = 80\,\text{MeV}$. Therefore, we can see that the maximum masses decrease as increasing the gap. If keeping the bag constant and gap fixed, the maximum masses of neutron stars with $m_s = 170\,\text{MeV}$ are larger than those with $m_s = 150\,\text{MeV}$. So increasing the strange quark mass makes the maximum masses of neutron stars increase because the EOS becomes stiffer. Specially, when we keep the parameters B and Δ fixed at reasonable values, we find that the maximum masses of neutron stars with CFL quark matter cores can be larger than $1.4M_\odot$ if $m_s \geq 180\,\text{MeV}$ (see fig. 6 or table 1). In this case it is difficult to judge a hybrid star from a neutron star only by a mass-radius relation according to the physics of neutron star summarized in ref. [15], *i.e.*, the presence of compact stars with CFL quark matter cores cannot be rule out. These results are also consistent with those obtained in refs. [16,17].

3.2 Conclusions

We have investigated the condensation of Goldstone bosons and the deconfinement phase transition from the HP to the CFL quark phase in neutron star matter. We use a chiral hadronic model called the FST model to describe the HP and the color-flavor-locked quark model to describe the quark phase. The conclusions are that the composition of neutron star matter is sensitive to the values of three free parameters in the CFL quark model: the bag constant B, the strange quark mass m_s and the color superconducting gap Δ. When $B^{1/4} = 190\,\text{MeV}$ is taken, the fractions of hadrons, leptons and π^--meson disappear and only the CFL quark matter with K^0 condensation exists in the high-density region in neutron star matter. Because the central densities of neutron stars are smaller than the critical densities of the pure CFL quark core, the hadronic-CFL mixed phase core exists in the center-of-neutron stars, while the pure CFL quark core is excluded. When we choose $B^{1/4} = 200\,\text{MeV}$, due to the appearance of hyperons, the critical density of the CFL quark matter is shifted to a higher density in the neutron star matter; because the critical density of the CFL quark matter is larger than the central density of neutron stars, the CFL quark matter cannot appear in neutron stars. The condensation of Goldstone bosons makes the pressure of the MP increase more smoothly during the transition. The K^0 condensation in the CFL phase has no remarkable influence on the EOS and properties of neutron star matter. In comparison with the unpaired quark matter, color superconductivity makes the EOS become softer, which results in smaller maximum masses of neutron stars. The EOS and properties of neutron star matter are also sensitive to B, m_s and Δ. Keeping Δ and m_s fixed, the EOS in the MP becomes softer and the maximum masses of neutron stars decrease with decreasing bag constant. When we fix the values of B and m_s, the larger value of the gap softens the EOS, which results in a smaller maximum masses of neutron stars. In the cases with the fixed values of B and Δ, increasing the strange quark mass makes the EOS stiffer and the maximum masses of neutron stars become larger.

This project was supported by the National Natural Science Foundation of China under grant Nos. 10575005, 10435080, 10425521, and 10135030, the Key Grant Project of the Chinese Ministry of Education (305001), and the CAS Knowledge Innovation Project (KJcx2-sw-No2).

References

1. N.K. Glendenning, *Compact Stars: Nuclear Physics, Particle Physics, and General Relativity* (Springer, New York, 2000).
2. F. Weber, J. Phys. G **25**, R195 (1999).
3. M.G. Alford, K. Rajagopal, J. Berges, Nucl. Phys. B **558**, 219 (1999).
4. T. Schafer, F. Wilczek, Phys. Rev. D **60**, 074014 (1999).
5. D.B. Kaplan, S. Reddy, Phys. Rev. D **65**, 054042 (2001).
6. P.F. Bedaque, T. Schafer, Nucl. Phys. A **677**, 802 (2002).
7. M.G. Alford, K. Rajagopal, S. Reddy, F. Wilczek, Phys. Rev. D **64**, 074017 (2001).
8. M.G. Alford, S. Reddy, Phys. Rev. D **67**, 074024 (2003).
9. P.K. Panda, D.P. Menezes, Phys. Rev. C **69**, 025207 (2004).
10. S. Banik, D. Bandyopadhyay, Phys. Rev. D **67**, 123003 (2003).
11. S. Banik, D. Bandyopadhyay, J. Phys. G. **30**, s525 (2004).
12. R.J. Furnstahl, H.B. Tang, B.D. Serot, Phys. Rev. C **52**, 1368 (1995).
13. J.F. Gu, H. Guo, R. Zhou, B. Liu, X.G. Li, Y.X. Liu, Astrophys. J. **622**, 549 (2005).
14. N.K. Glendenning, Phys. Rev. D **46**, 1274 (1992).
15. J. Lattimer, M. Prakash, Science **304**, 23 (2004).
16. M. Alford, D. Blaschke, A. Drago, T. Klähn, G. Pagliara, J. Schaffner-Bielich, astro-ph/0606524.
17. M. Alford, M. Braby, M. Paris S. Reddy, Astrophys. J. **629**, 969 (2005).